Deep-Sea Research Part I xxx (xxxx) xxx–xxx

Contents lists available at ScienceDirect

Deep-Sea Research Part I

journal homepage: www.elsevier.com/locate/dsri

Decadal variability in coastal phytoplankton community composition in a changing West Antarctic Peninsula

Oscar Schofield[a,*], Grace Saba[a], Kaycee Coleman[a], Filipa Carvalho[a], Nicole Couto[a], Hugh Ducklow[b], Zoe Finkel[c], Andrew Irwin[c], Alex Kahl[a], Travis Miles[a], Martin Montes-Hugo[d], Sharon Stammerjohn[e], Nicole Waite[a]

[a] Rutgers University's Center for Ocean Observing Leadership (RU COOL), Department of Marine and Coastal Sciences, School of Environmental and Biological Sciences, Rutgers University, New Brunswick, NJ 80901, USA
[b] Lamont-Doherty Earth Observatory, Palisades, NY 10964, USA
[c] Mount Allison University, Sackville, NB, Canada
[d] Institut des sciences de la mer de Rimouski, Université du Québec à Rimouski, 310 allée des Ursulines, Rimouski, Québec, Canada G5L 3A1
[e] Institute of Arctic and Alpine Research, University of Colorado, Campus Box 450, Boulder, CO 80309-0450, USA

ABSTRACT

The coastal waters of the West Antarctic Peninsula (WAP) are associated with large phytoplankton blooms dominated by large (> 20 μm) diatoms however, nanoplankton (< 20 μm) are also an important component of the food web. The dominant nanoflagellates in the WAP are cryptomonad algae. Using a twenty-year time series collected by the Palmer Long Term Ecological Research program at the United States Palmer Research Station, we assessed long-term patterns and stability in the coastal phytoplankton communities in the WAP. There was significant interannual variability in the integrated water column chlorophyll *a* (chl-*a*) concentrations, which varied by a factor of 5 over the 20-year time series. There has been a significant positive increase in the seasonally integrated concentration of chl-*a* over the time series. The dominant phytoplankton were diatoms, with cryptophytes the second most abundant. Mixed flagellates also constituted a significant fraction of the chl-*a* but showed less interannual variability than diatoms and cryophytes. Peak phytoplankton biomass was observed in summer months, when monthly averaged wind speed was lower than in the fall and autumn. Cryptophytes were most abundant during the summer months (December-January) after the seasonal retreat of sea ice. While diatoms were observed over the full range of observed salinities 32–34.5) as well as over the full range of *in situ* temperatures (−1.5 to 2.5 °C), the cryptophyte populations were observed in locations with lower salinity 32.5–33.75) and colder water (−1 to 1 °C). Environmental factors that favored a shallower seasonal mixed layer resulted in larger diatom blooms compared to the other phytoplankton taxa. During summer with lower phytoplankton biomass, a larger proportion of the chlorophyll *a* was associated with cryptophytes. These results demonstrate that continued temperature changes along the West Antarctic Peninsula will result in changes in phytoplankton concentration and community composition, which has significant ramifications for the food web.

1. Introduction

The West Antarctic Peninsula (WAP) is experiencing some of the fastest rates of regional change on Earth (Clarke et al., 2007; Schofield et al., 2010). The changes in the WAP are profound with mid-winter surface atmospheric temperatures increasing by 6 °C (> 5x the global average) over the last 50 years (Skvarca et al., 1999; Vaughan et al., 2003; Turner et al., 2005). Eighty-seven percent of the WAP glaciers are in retreat, the annual sea ice season has shortened by 90 days, and perennial ice is no longer a feature of the northern WAP (Cook et al., 2005; Martinson et al., 2008; Stammerjohn et al., 2008). Additionally, warmer winters are associated with increased cyclonic circulation with an associated increase in warm air advection, resulting in increased precipitation at the WAP in recent decades (Thomas et al., 2008). These changes appear to be accelerating (Rignot et al., 2008) and while these decadal changes remain within natural climate variability, so it cannot yet be ascribed to anthropogenic driven change (Turner et al., 2016), it is a unique model system to study how future changes might ripple through polar ecosystems.

Ocean warming has been implicated as a major driver for the

* Corresponding author.
E-mail address: oscar@marine.rutgers.edu (O. Schofield).

http://dx.doi.org/10.1016/j.dsr.2017.04.014
Received 19 November 2015; Received in revised form 27 March 2017; Accepted 24 April 2017

deglaciation (Vaughan et al., 2003) through the upwelling of the heat delivered by relatively warm (~2 °C) Upper Circumpolar Deep Water (UCDW). The UCDW is derived from the Antarctic Circumpolar Current that flows along the continental slope of the WAP (Klinck, 1998). The increased presence of the UCDW on the continental shelf has been associated with an increasing trend in the Southern Annular Mode (SAM) that has increased westerly winds and has been linked to a rise in the ocean heat flux (Martinson et al., 2008). The net change in sea-ice cover has been suggested to underlie observed changes in the coastal ecosystems of the WAP (Smith et al., 1999; Ducklow et al., 2007).

The coastal waters of the WAP are associated with large phytoplankton blooms that are dominated by diatoms (Hart, 1942; Nelson and Smith, 1991; Prézelin et al., 2000, 2004; Smith et al., 2008). The high phytoplankton productivity is fueled by an ample supply of nutrients and the availability of light when the mixed layer depths (MLD) are shallow allowing cells to overcome light limitation (Mitchell and Holm-Hansen, 1991; Venables et al., 2013). Macronutrients are highly abundant throughout the WAP (Serebrennikova and Fanning, 2004; Ducklow et al., 2012; Kim et al., 2016) and although they show marked seasonality (Clarke et al., 2008a, 2008b), in most cases they do not appear to limit phytoplankton growth (Holm-Hansen and Mitchell, 1991; Kim et al., 2016) except during very large blooms. The high productivity supports a productive food web that is tightly coupled to the seasonal phytoplankton dynamics suggesting strong bottom-up control of the system (Saba et al., 2014). Over the past 30 years, there is evidence that the magnitude of phytoplankton blooms in the WAP have changed (Montes-Hugo et al., 2009). The changes have been particularly dramatic in the northern WAP, with a decline in chlorophyll *a* associated with an increase in cloudy days, deepening upper mixed layer depth, stronger intensity winds, and shorter sea ice seasons along the marginal ice zone (Montes-Hugo et al., 2009). In contrast to the northern sectors of the WAP, the southern areas have experienced increasing phytoplankton biomass over time. Montes-Hugo et al. (2009) argued these increases reflected an increase in the duration and area of ice free water during the summer season.

Phytoplankton blooms in the WAP are dominated by large (> 20 μm) diatoms (Hart, 1942; Holm-Hansen and Mitchell, 1991); however over the last three decades the traditional paradigm has been revised recognizing that nano- (< 20 μm) and picoplankton (< 2 μm) are a critically important component to the WAP phytoplankton community (Whitaker, 1982; Krebs, 1983; Hewes et al., 1990; Buma et al., 1991; Jacques and Panouse, 1991, Villafañe et al., 1993). The dominant nano-flagellates in the WAP appear to be cryptophytes (Krebs, 1983; Whitaker, 1982; Kopczynska, 1992; Garibotti et al., 2003; Mura and Agusti, 1998; Varela et al., 2002; F. Rodriguez et al., 2002a; J. Rodriguez et al., 2002b). Numerous field programs have documented that cryptophytes are often spatially and temporally segregated from the diatom communities (Garibotti et al., 2003; F. Rodriguez et al., 2002a; J. Rodriguez et al., 2002b; Moline et al., 2004, Garibotti et al., 2005). Cryptophyte populations are often associated with either mid-shelf fronts (Mura and Agusti, 1998) or low salinity surface plumes (Mura et al., 1995; Moline et al., 2004). This has led to the hypothesis that cryptophyte communities will grow in importance in the WAP food web as sea and glacial ice melt will increase the spatial extent of low salinity water (Moline et al., 2004).

To date, the majority of the studies have been based on ship and/or field station efforts conducted for a limited duration (1–3 field seasons) thus providing snapshots of the ecosystem at any given time. For this study we analyzed a twenty-year time series collected by the Palmer Long Term Ecosystem research (Pal LTER) program at the United States Palmer Research Station to assess long-term ecological patterns and stability in the coastal phytoplankton communities in the WAP. Our results confirm that diatoms and cryptophytes are the dominant phytoplankton groups and are inversely related to each other; however mixed flagellates are also a significant fraction of the phytoplankton community. At Palmer Station the presence of the cryptophytes is associated with lower temperature and lower salinity water associated with the sea ice and glacial melt. We observe, since 2009, increasing sea ice at Palmer Station along with increased seasonal concentrations of chlorophyll. These increases are associated with an increasing proportion of diatoms with the phytoplankton community, which should be favorable for the Antarctic krill.

2. Materials and methods

Data was collected as part of the Palmer Long Term Ecological Research (LTER) project, which was initiated in 1991 to study how annual sea ice variability structures the ecology and biogeochemistry of the West Antarctic Peninsula (WAP). The project was established before it was appreciated that this region was undergoing significant change associated with a warming atmosphere. The data is publicly available through the Palmer LTER data system (http://pal.lternet.edu/data).

2.1. Sea ice characterization

Sea ice data were calculated using Version 2 of the Bootstrap sea ice concentrations from Nimbus-7 SMMR and DMSP SSM/I that are referenced to daily tie-points consistent with the AMSR-E Bootstrap algorithm. GSFC Bootstrap time series data (version 2.0) for 1/1979 to 10/2010, supplemented by preliminary Near-Real-Time-Sea-Ice (NRTSI) data (using the NASA Team algorithm) for Nov-Dec 2010. Sea ice duration is defined as the time elapsed between day of advance and day of retreat within a given sea ice year, which begins mid-February (mean minimum of summer sea ice extent for the Southern Ocean) and ends the following mid-February. Imagery from a 50 km area south and west of Anvers Island was used for this manuscript and assumed to be representative of Palmer LTER sampling area. See Stammerjohn et al. (2008) for further details.

2.2. Seawater sampling

The Palmer LTER program has carried out sampling at Palmer Station (−64.8° South, −64.1° West) in the austral spring-summer annually since December of 1991 (Fig. 1). The sampling locations at Palmer Station are an inshore station B (bottom depth ≈75 m) and an offshore station E (bottom depth ≈200 m) (Fig. 1), both of which are within Adélie penguin foraging areas (Oliver et al., 2013), which is a central focus for the LTER (Schofield et al., 2013). Station E is located offshore at the edge of the Palmer Station boating limit and has a distinct marine signature associated with Palmer Deep Canyon, which is a seafloor conduit hypothesized to allow the inputs of modified UCDW (Schofield et al., 2013; Carvalho et al., 2016). Station B is adjacent to the Marr Glacier. Despite these differences, phytoplankton biomass and community composition from Stations B and E are highly correlated (Fig. 2). The one difference is that overall phytoplankton concentrations were consistently higher in the nearshore waters at Station B (Fig. 2).

The goal of the Palmer LTER is to sample stations B and E twice per week from mid-/end of October to mid-/end March. Sampling at each station is conducted *via* Zodiac where a CTD is lowered manually for a vertical profile of water column physics, and is immediately followed by a Go-Flo bottle cast to collect seawater at selected depths for phytoplankton (*i.e.*, chlorophyll *a* [chl-*a*], phytoplankton pigments, primary productivity). Seawater from each depth is stored in dark amber Nalgene bottles and processed immediately upon returning to the laboratory at Palmer Station. Zodiac sampling in this region is heavily dependent on weather, sea ice, time, and personnel availability. Thus, data gaps exist within the time series, as some seasons had limited or irregular sampling as well instrument issues in the early years. Data exist for all years except 2007–08. Nonetheless, the summer months of December, January, and February (DJF) were the most consistently sampled. When data were available for the full sampling season (Oct – Mar), the depth-integrated mean chl-*a* during DJF was always higher

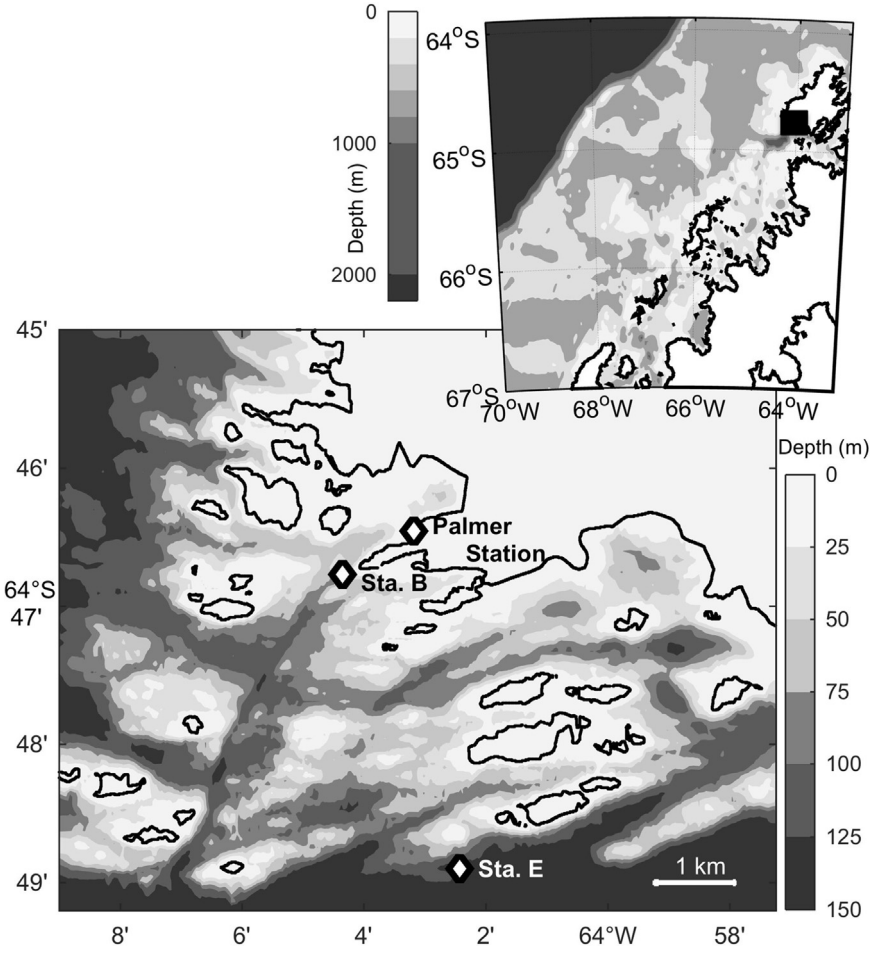

Fig. 1. Study site for LTER research at Palmer Station, which is located on the West Antarctic Peninsula. Data for this study was collected at Stations B and E.

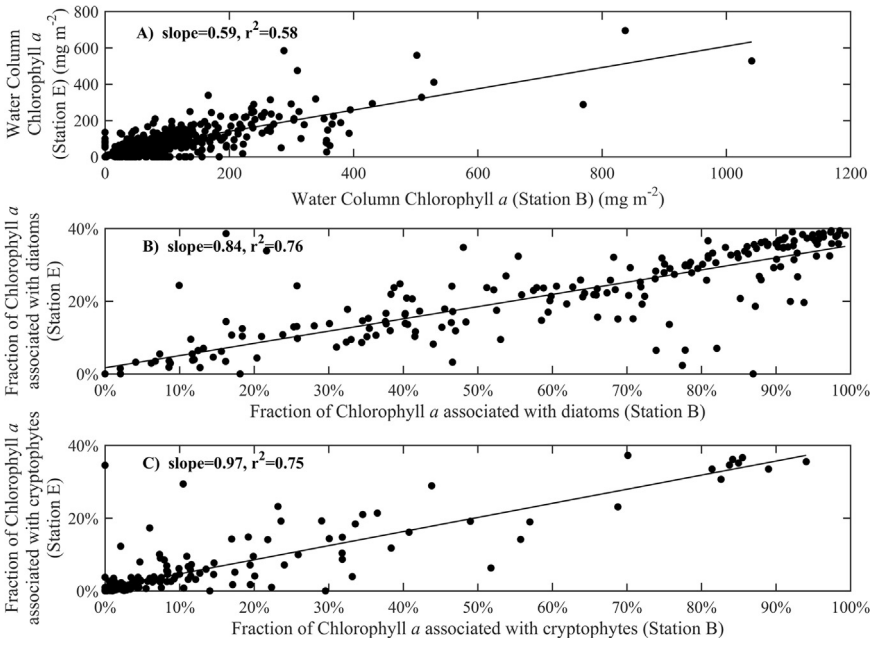

Fig. 2. The correlation between the monthly mean phytoplankton biomass and community composition between Stations B and E. A) The correlation for water column integrated chlorophyll-*a* (chl-*a*) was highly significant ($p \ll 0.01$, $R^2 = 0.58$). B) The correlation for the relative fraction of chl-*a* associated with diatoms was highly significant ($p \ll 0.01$, $R^2 = 0.84$). C) The correlation between the relative fraction of chl-*a* associated with cryptophytes was highly significant ($p \ll 0.01$, $R^2 = 0.75$).

than when all other months (Oct – Mar) were pooled together, suggesting that maximum phytoplankton biomass typically accumulated in summer. Thus, we considered DJF representative of the biological summer season and we used these months to estimate seasonal averages of biological data. Higher resolution studies of the phytoplankton dynamics were studied using Slocum gliders and results are described in Carvalho et al. (2016). Data collected by the Palmer LTER project is available at http://pal.lternet.edu/data/.

2.3. Chlorophyll-a and accessory pigments

Seawater collected at different depths was filtered (1–2 L) onto 25 mm GF/F filters, wrapped in foil, and frozen at −80 °C for fluorometric phytoplankton chlorophyll-*a* (chl-*a*) analysis (mg chl-*a* m^{-3}) or flash frozen in liquid nitrogen and stored at −80 °C for HPLC pigment/phytoplankton composition analysis (mg pigment m^{-3}). Generally, eight depths were collected for each profile, with the several depths chosen based on the characteristics of the depth profiles collected by the CTD. Filters were extracted in 90% HPLC grade acetone for 24 h after being macerated with either Teflon pestle and being ultrasonicated. Samples pre-filtered through another GF/F (1995–2001) or through a 0.45 mm Whatman nylon Puradisk filter (2006–2009) before injection. Procedures and gradients for the HPLC procedures are described in Kozlowski et al. (2011). For this study, chl-*a* and HPLC pigment data was integrated to 50 m water depth that consisting of 7–8 samples collected in the upper water column.

The taxonomic composition of the phytoplankton assemblages was derived quantitatively from a High Performance Liquid Chromatography (HPLC) analysis of pigment data using CHEMTAX (V195) with initial pigment ratios derived from WAP phytoplankton by Kozlowski et al. (2011). While diatoms and cryptophytes have definitive marker pigments, “mixed flagellates” represent a range of taxa that includes dinoflagellates and unidentified phytoflagellates. For each vertical profile, we calculated the depth-integrated chl-*a* and accessory pigments (mg m^{-2}) in the upper 50 m of the watercolumn. Sampling in five seasons (1993/1994, 1994/1995, 2001/2002, 2003/2004, 2004/2005) had few vertical profiles that extended to 50 m. For these profiles we integrated to the deepest depth sampled (median = 40 m); thus, depth-integrated chl-*a* and accessory pigments were likely slightly underestimated. Seasonal accessory pigment and chl-*a* averages were calculated using only DJF data. The HPLC instrument used by the program was damaged in shipping in 2009 which has lead a to delay in the sample processing. Thus HPLC data only through 2008 is presented.

2.4. Primary productivity

The primary productivity rates were measured by the uptake of radioactive sodium bicarbonate. In borosilicate flasks, 100 ml aliquots of the sea-water, collected by the CTD at selected depths (at minimum 5 depths), were inoculated with nominally 1 μCi of $NaH^{14}CO_3$ per bottle. Integrated rates were calculated for the upper 50-meters of the water column. The borosilicate bottles were incubated for 24 h with bottles screened to *in situ* light levels. Given the bottles were not UV-transparent, these photosynthesis rates should be considered upper limit estimates. Samples were incubated in an outdoor deck incubator that was plumbed to the Palmer Stations seawater system, maintaining samples at ambient temperatures. After incubation, samples were filtered onto GF/F filters, washed with 10% HCl, dried and counted in a scintillation counter.

2.5. Water column stability/stratification parameters

Over the course of the program, physical oceanographic data (temperature and conductivity as a function of pressure) was collected using several instruments. From 1991 to 2007, a SeaBird Elecronics (www.seabird.com) Seacat SBE 19 was used. From 2007 onward a SeaBird Elecronics Seacat SBE 19plus was used, though not in field season 2008–2009. We accounted for sensor drift using calibrations made before and after each field season, following methods recommended by SeaBird, assuming linear drift for sensors. We used SeaBird's standard software functions to process the data, removing effects for zodiac heave (pressure reversals), and to ensure that the temperature, conductivity and pressure were measured on the same water parcel. Data was averaged into 2 db pressure bins for the older SBE19 data and 1 db bins for the newer instrument, which samples at twice the frequency. Conductivity data was then converted to salinity. From 2008 until 2011, a Falmouth Scientific Inc. FSI MCTD-3 and a Satlantic HyperPro-II (which includes temperature, conductivity and pressure ancillary sensors) were also used to collect physical oceanographic data. As much as possible, we followed the same methods to process this data. The three instruments combined provided full data coverage every time water samples were collected. Plots of each cast were inspected visually and in relation to other casts to look for any issues with the data (eg, bad surface values due to sea-state). These values were removed from the data set.

In order to define an ecologically relevant seasonal mixed layer (MLD), we used the approach described in Carvalho et al. (2017). For each profile, surface MLD is estimated by finding the depth of the maximum water column buoyancy frequency, or max(N^2). Because this method is focused on the water column vertical structure, a Quality Index (QI) filter is also applied to identify water column profiles without significant stratification. For this we used QI (Eq. (1)) developed by Lorbacher et al. (2006) to evaluate individual MLD calculations against water column density and filter out profiles where MLD could not be resolved. The QI is calculated as:

$$QI = 1 - \frac{rmsd\,(\rho_k - \overline{\rho})\,|_{(Z_1, Z_{MLD})}}{rmsd\,(\rho_k - \overline{\rho})\,|_{(Z_1, 1.5\times Z_{MLD})}} \quad (1)$$

where ρ_k is the density at a given depth (k), Z_1 is the first layer near the surface and rmsd() denotes the standard deviation from the vertical mean $\overline{\rho}$ from Z_1 either to the MLD or 1.5xMLD. This index evaluates the quality of the MLD computation. Using this, MLDs can be characterized into estimates determined with certainty (QI > 0.8), determined but with some uncertainty (0.5 < QI < 0.8) or not determined (QI < 0.5). Following the thresholds set by Lorbacher et al. (2006), for the analyses presented in this study, a quality index of 0.5 was used to reasonably warrant a calculation of MLD. Some summer seasons had sparse sampling, less than 6 profiles collected over the season, which we omitted from the QI analyses.

This determination of MLD is based on the principle that there is a near-surface layer characterized by quasi-homogeneous properties and where the standard deviation of the property within this layer is close to zero. Below the MLD, the variance of the property should increase rapidly and is identified as the peak of the variance in the upper water column. This method does not consider the strength of stratification, just homogeneity of the surface layer present. Therefore, by definition MLD estimate is close to the lower boundary of that vertically uniform layer. The method was validated for three locations across the Southern Ocean (WAP, Amundsen, Ross Sea) and it ecological relevance was confirmed against independent chlorophyll data (Carvalho et al., 2017).

3. Results

It is well documented that the West Antarctic Peninsula (WAP) has been experiencing changes in the sea ice duration and extent (Stammerjohn et al., 2008) which is also true for the Palmer Station region (Fig. 3). Despite significant interannual variability, the timing of sea ice retreat in the Palmer region has been occurring earlier over time (Fig. 3A). Sea ice retreat in the early nineties often occurred in the month of December, but after declines from 2006 through 2009, sea ice retreat occurred as early as mid-September. Since 2009, the timing of

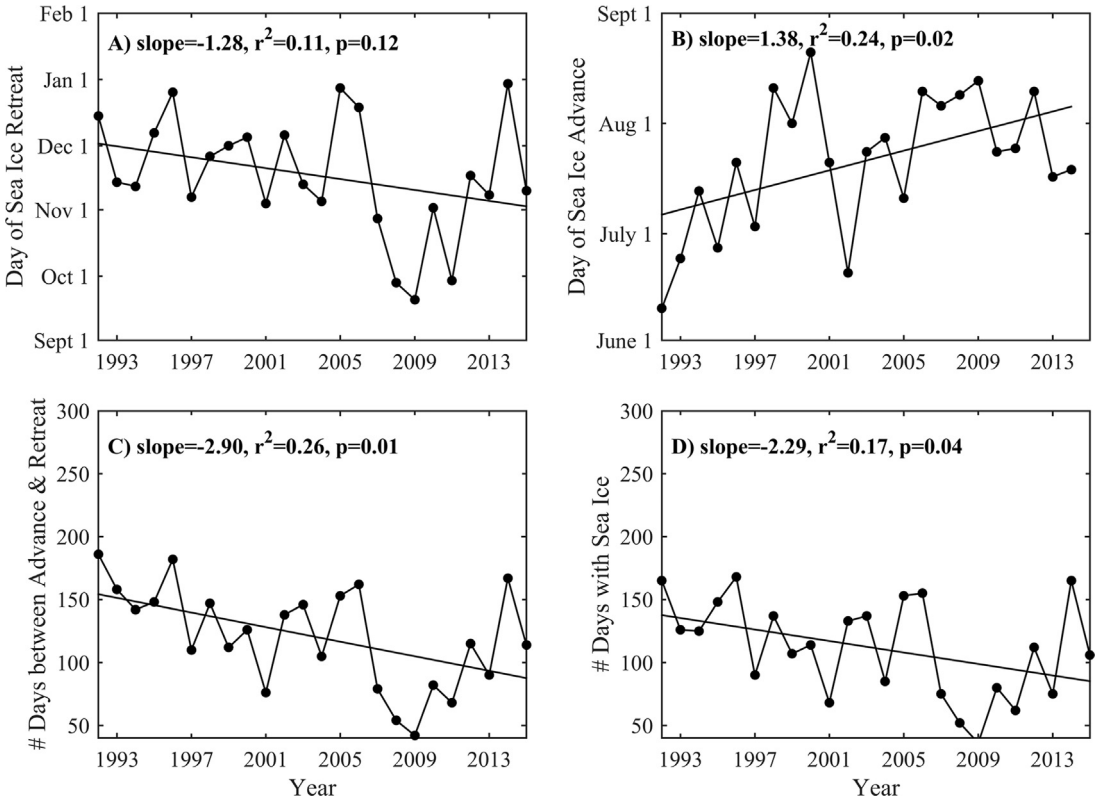

Fig. 3. Changes in annual sea ice dynamics near Palmer Station. A) Time series of the day of sea ice retreat. B) Time series of the number of days of sea ice advance. There was a significant ($p = 0.02$) positive trend over time. C) The time series variability of the days between of sea ice advance and retreat. There has been a significant decrease ($p = 0.02$) in the day of sea ice advance in the Palmer Station station region. D) The interannual variability in the number of sea days. The number of sea ice days has significantly ($p = 0.04$) decreased over the last 2 decades.

sea ice retreat has rebounded and now most often occurs in mid-November. Sea ice advance also has exhibited significant change with sea ice advance occurring later by almost 2 months during the year (Fig. 3B). Sea ice retreat shows larger interannual variability than sea ice advance. The net result is that over the last two decades the number of days between sea ice advance and retreat (Fig. 3C) and total of sea ice days (Fig. 3D) have shown significant ($p < 0.05$) declines.

The coastal waters around Palmer Station exhibit significant interannual variability in phytoplankton biomass. Integrated water column chl-*a* concentrations varied by a factor of 5 over the 20-year time series at Palmer (Fig. 4A). Values ranged from ~100 to over 500 mg chl-*a* m^{-2}. Seasonally integrated chl-*a* anomalies show an increasing trend (Station B: $R^2 = 0.38$, $p = 0.01$; Station E- $R^2 = 0.24$, $p = 0.01$) over the last two decades (Fig. 4B). In recent years there were two years 2009/2010 and 2012/2013 that exhibited large week-long chl-*a* blooms during the summer that resulted in a 2–3 fold higher seasonal variance in the chlorophyll biomass (Fig. 4C). The shifts from generally lower chl-*a* biomass in the 1990's and early 2000's to higher chl-*a* values in the later years of the time series were associated with a shallower seasonal mixed layer depth (SMLD) (Fig. 4B). These was a significant inverse correlation ($p = 0.04$) between the seasonal averaged summer mixed layer depth and the integrated summer chl-*a* (Fig. 5). The SMLD could account for 27% of the variance in the integrated chl-*a* (Fig. 5). While the seasonal and depth integrated chl-*a* was not correlated with the days of sea ice retreat (Fig. 6A) and advance (Fig. 6B), there was significant inverse correlations with the number of days between sea advance and retreat (Fig. 6C, $p = 0.00$) as well as number of days of sea ice (Fig. 6D, $p = 0.01$).

Combining the CHEMTAX outputs with measured chl-*a* allowed estimation of the amount of chl-*a* for the major phytoplankton taxa to be estimated. The most dominant phytoplankton taxa present in the waters near Palmer Station were diatoms, which each year accounted for over 90% of the chl-*a* at both Stations B and E (Fig. 7A). Water column integrated chl-*a* associated with diatoms often exceeded 200 mg m^{-2}, which was significantly higher than the chl-*a* associated with other major phytoplankton taxa (Figs. 7B-E). This was consistent with the observation that the concentration of accessory pigment fucoxanthin, associated with diatoms, could account for up to 60% of the variability in the concentration of chl-*a* ($p = 0.005$). The next most abundant phytoplankton taxa were the cryptophytes and mixed flagellates (Figs. 7B, C). Cryptophyte populations peaked at ≥50% of the chl-*a* in 8 of the 20 years. Six of the years had > 50 mg chl-*a* m^{-2} associated with cryptophytes. Mixed flagellates were also a significant component to the phytoplankton community consistently accounting for ~50 mg chl-*a* m^{-2} (Fig. 7C). Prasinophytes were present throughout the time series consistently accounting for < 10 mg chl-*a* m^{-2} except for 2001 and 2008 (Fig. 7D). Similar to the prasinophytes, the type-4 haptophytes concentrations were consistently 10–20 mg chl-*a* m^{-2} (Fig. 7E). Despite significant interannual changes in phytoplankton communities, the chlorophyll-normalized ^{14}C productivity was relatively consistent over the time series (Fig. 7F).

The monthly mean in phytoplankton concentration and community composition during summer months was assessed over the time series for each of the summer months (Fig. 8). Monthly averaged water-column integrated chl-*a* concentrations, using the full data set, showed increasing concentrations in November and December, which then peaked in January before declining in February (Fig. 8A). It should be noted that biomass levels were already detectable in November suggesting that favorable conditions began early in the summer season. While the overall water column concentration of chl-*a* was higher in the nearshore waters of station B compared to Station E, the seasonal behavior was similar (Fig. 8A). The increase in chl-*a* mirrored the declining monthly mean wind speed measured at Palmer Station during the summer months. Peak chlorophyll concentrations coincided with a

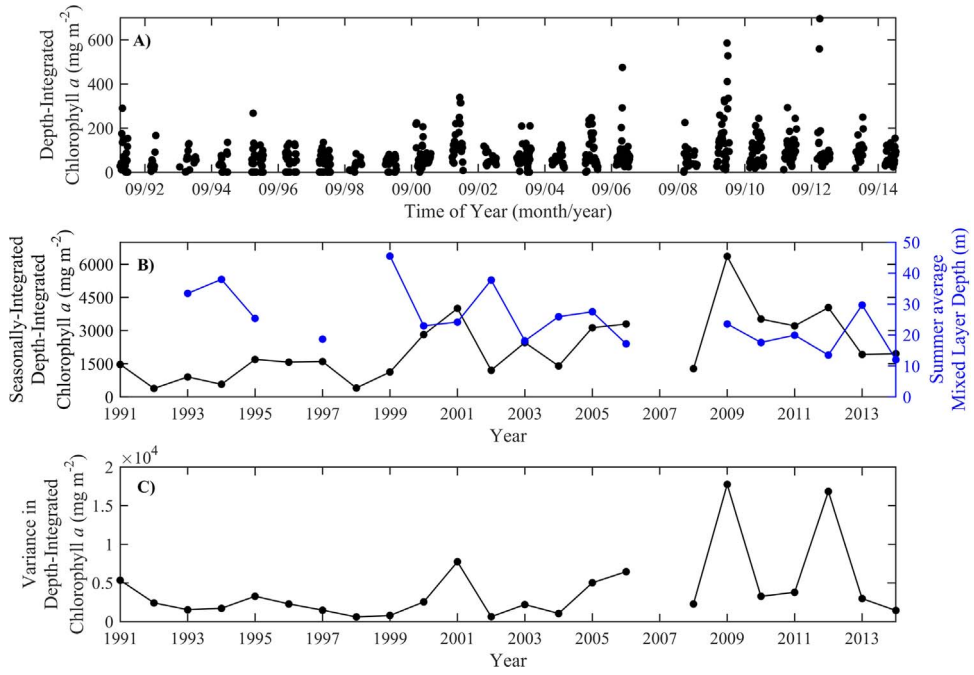

Fig. 4. The interannual variability chlorophyll *a* at Station E. A) The internanual variability in the water column integrated water column chlorophyll *a* (mg chl *a* m^{-2}). Data was only collected during the austral summer months. B) The inter-annual seasonally-integrated water column chl *a* from Station E. The seasonally integrated data shows a positive trend over the last two decades ($p = 0.004$). Overlaid in blue are the summer season average mixed layer depth. Missing years in the mixed layer were when there were fewer the 6 profiles for that season. C) The time series of the variance in depth and seasonally integrated chl-*a*. The relationship was positive and heavily weighted by the later years in the time series but was not significant ($p = 0.09$). (For interpretation of the references to color in this figure legend, the reader is referred to the web version of this article).

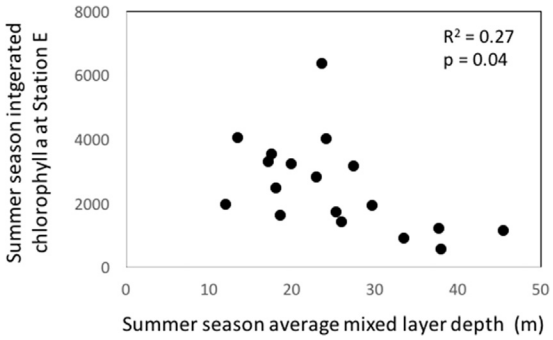

Fig. 5. The correlation between summer integrated chlorophyll *a* at Station E with the summer averaged mixed layer depth. There was a significant inverse relationship between the chl-a and mixed layer depth ($p = 0.04$).

minimum monthly average wind speed at around 7 knots (Fig. 8A). The declining wind speed was coincident with increasing seasonal solar illumination. While the diatoms and cryptophytes, the two major phytoplankton taxa in these waters, showed changes during the summer months, the background phytoplankton populations (mixed flagellates, haptophytes, and prasinophytes) did not show any significant change over the summer months (Fig. 8B). Diatoms dominated the early and late summer accounting for 72% and 68% of the monthly chl-*a* in the months of November and February respectively (Fig. 8B). The contributions of the cryptophytes were highest in the months of December and January, where on average they accounted for 24% and 20% of the chl-*a* (Fig. 8B). To assess the quantitative relationship between the diatoms and cryptophytes (CHEMTAX provides the relative relationship), we compared the concentrations of alloxanthin (cryptophyte chemotaxonomic pigment) and fucoxanthin (diatom chemotaxonomic pigment). Cryptophyte and diatom blooms were not found to coincide (Fig. 9A). This was not as clear comparing the fucoxanthin with the major pigment marker for mixed flagellates (19′-butanoyloxyfucoxanthin, Fig. 9B). Highest concentrations of chl-*a* were associated with diatom populations.

Histograms of the frequency of the occurrence for the major phytoplankton groups (diatoms, cryptophytes and mixed flagellates) against air temperature, water depth, and mixed layer depth are presented in Fig. 10. The three taxa were found at distinct air temperature, water depths. All three of the phytoplankton taxa were skewed to air temperatures above the 0 °C. Peak diatom abundance was found at the lowest mean air temperature of 1.20 °C (Fig. 10A). Peak mixed flagellates were on average associated with an air temperatures of 1.39 °C and the cryptophytes were associated with the warmest air temperature at 2.32 °C (Fig. 10A). Peak cryptophyte abundance was associated with the shallowest mean water depth of 10.23 m (Fig. 10B). The diatoms were on average associated with a mean water depth of 15.09 m (Fig. 10B). Mixed flagellate abundance was associated with the deepest depth of 17.60 (Fig. 10B). Mixed flagellates were found at the deepest MLD (17.55 m) consistent with what appeared as a consistent background population throughout the time series. Diatoms were found in greatest number at a MILD of 15.14 m, with cryptophytes found most often at the shallowest MLD of 14.11 m. This is consistent with the cryptophytes associated with shallow, lower salinity waters (see below). Overall the results suggest evidence of niche segregation between the diatoms, cryptophytes, and mixed flagellates.

The dominant groups were associated with specific water masses (Fig. 11). Diatoms and cryptophytes were separated in temperature-salinity phase space for Stations B and E (Fig. 11). Significant concentrations of diatoms were observed over the full range of observed salinities (34.5 to 32) as well as over the full range of *in situ* temperatures (−1.5 to 2.5 °C) (Fig. 11A). Significant diatom concentrations were absent from colder (−1 to 1 °C) and lower salinity (33.75 to 32.5) water (Fig. 11A). Peak cryptophyte populations were observed in lower salinity (33.75 to 32.5) and colder water (−1 to 1 °C) (Fig. 11A). Cryptophyte populations were absent at higher temperatures (> 1 °C) and salinities > 33.75. Mixed flagellates like the diatoms were observed over all temperatures and salinities however in general peak abundances were not encountered at low temperature and salinity (Fig. 11B).

During the time series (1991–2012), peaks in depth-integrated

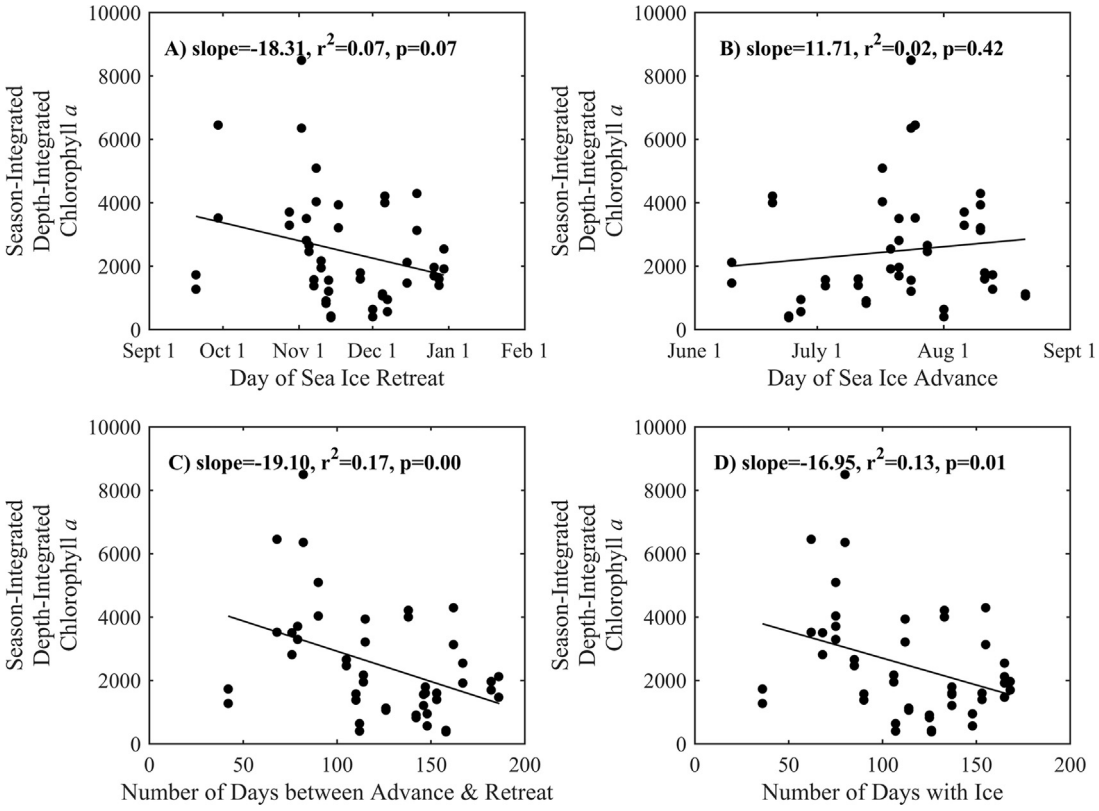

Fig. 6. The relationships between seasonally and water column integrated chl-*a* with the dynamics in sea ice. A) There was no significant (p = 0.07) relationship between chl-*a* and the annual day of sea ice retreat. B) There was no significant (p = 0.42) relationship between the days of sea ice advance and the depth and seasonally integrated chl-*a*. C) The relationship between the depth-seasonally integrated chl-*a* and the number of days between sea ice advance and retreat which showed a significant (p = 0.009) negative relationship *a*. D) The correlation between the number of sea ice days and the seasonally integrated chl-*a*. There was a significant (p = 0.01) negative relationship between these parameters.

(0–50 m) summer chl-*a* concentration occurred, on average, every 4–6 years (Fig. 12, Saba et al., 2014). The relative phytoplankton composition (as determined by CHEMTAX) during peak chl-*a* years was dominated by diatoms, whereas the proportion of cryptophytes increased in low chl-*a* years (Fig. 12) (one-way analysis of variance, $P < 0.001$). The relative concentrations of the other phytoplankton taxa did not show significant changes during the high and low chl-*a* years (Fig. 12). Summers with high chlorophyll concentrations were associated with years of high abundances of diatoms and cryptophytes. We observed significant correlations between the SMLD and integrated summer chl-*a*. While high chlorophyll years were associated with a relative increase in the diatoms over other phytoplankton groups (Fig. 12), high chlorophyll anomaly years were positively correlated with the amount of the chl-*a* associated with both diatoms and cryptophytes (Fig. 13). The chl-*a* anomaly of the diatoms was significantly positively correlated with the chlorophyll anomaly ($p < 0.01$, Fig. 13A). The high chlorophyll anomaly could explain 39% of the variability in diatom anomaly. Cryptophyte chlorophyll anomalies were also positively associated with high chl-*a* (p = 0.03, Fig. 13B). The similarities between the two correlations (Figs. 13A and B) reflect that diatoms and cryptophytes were the most abundant phytoplankton groups. Given that these populations did not co-occur (Fig. 9), the respective blooms of the diatom and cryptophytes must have occurred at different times of the summer season. There was no significant relationship between the mixed flagellates and the chlorophyll anomalies (Fig. 13C).

4. Discussion

The WAP has been exhibiting significant change over the last decade (Stammerjohn et al., 2008; Montes-Hugo et al., 2009; Ducklow et al., 2012); however the relative change in the physics, chemistry, and the biology varies latitudinally (Ducklow et al., 2012). Based on a satellite analysis Palmer station is located in the transition zone between the warmer maritime conditions associated with declining chl-*a* in the northern WAP and the more polar continental conditions associated with increasing chl-*a* in the south (Montes-Hugo et al., 2009). Increasing chl-*a* in the southern waters of the WAP have been hypothesized to reflect the increased periods of open water due to reduced sea ice coverage in the spring and summer. Our results suggest the same is true at Palmer Station where the number of sea ice days are inversely related to the amount of summer chl-*a*. While for much of the time series at Palmer there was a decline in the numbers of days of sea ice each year, there recently has been a change with a significant increase in sea ice. Associated with the increasing sea ice has been the increase in the amount of summer chl-*a* at Palmer. The Montes-Hugo et al. (2009) analysis did not include recent changes as it compared the changes between 1978–1986 and 1998–2006, well before the recent increases in chl-*a* and sea ice began after 2009. While there was an increase in sea ice, the summer months at Palmer still remain relatively ice free and the primary factor influencing the bloom is depth of the summer mixed layer depth which is most likely regulated to local wind forcing and circulation patterns. These forcing factors are augmented by factors that have occurred before the summer. The total amount of sea ice/glacial melt in the spring can help stabilize the water with a surface layer of lower saline water. Saba et al. (2014) found that winters that had significant sea ice were associated with shallower and more stable seasonal upper mixed depth in the spring. High ice extent in the winter likely facilitated higher stratification in the following spring and summer *via* two mechanisms, 1) insulation the water column from high winter winds through much of the spring thus preventing the formation of a deep winter mixed layer (Montes-Hugo et al., 2009; Venables et al., 2013) and 2) providing a larger volume of sea ice melt water that strengthens the density gradient in the upper water column

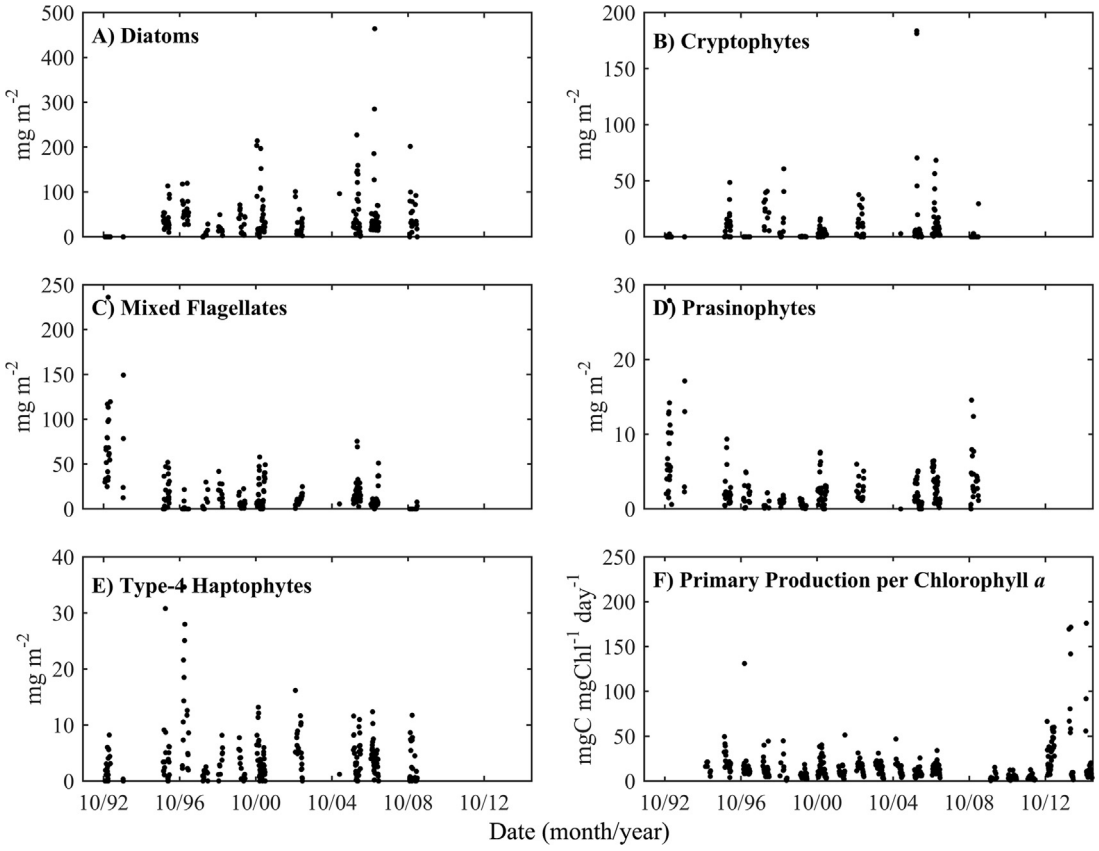

Fig. 7. The interannual variability in the chlorophyll concentrations associated with the major phytoplankton taxa at Station E near Palmer Station derived from CHEMTAX and *in situ* chlorophyll concentrations. A) The internannual variability of the chl-*a* associated with diatoms. B) The internannual variability of cryptophytes. C) The internannual variability of mixed flagellates. D) The internannual variability of prasinophytes (note scale change in y-axis) of chl-*a*. E) The internannual variability of type-4 haptophytes (note scale change in y-axis). F) Variability in the 14C-daily carbon fixation rates normalized to chl-*a*.

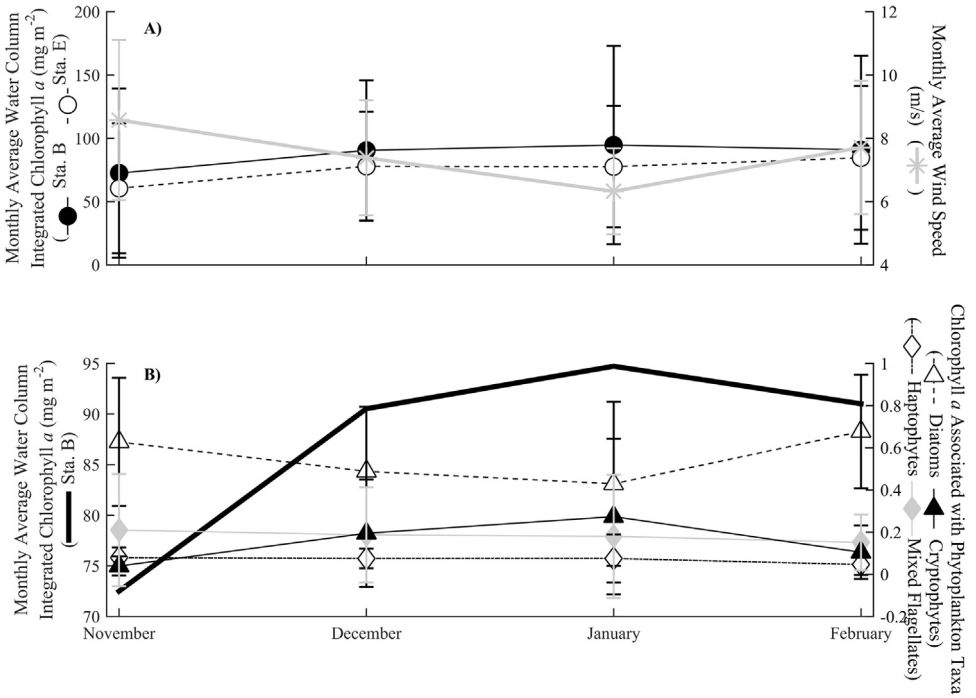

Fig. 8. Mean summer dynamics in phytoplankton biomass and community composition. A) The monthly mean for the full 20-year time series for wind speed measured at Palmer station (grey line) and water column chl-*a* concentrations at Station B (black circle and line) and Station E (open circle and dashed line). The standard deviations for the monthly wind speed and chl-*a* are shown. B) The monthly mean for the full 20-year time series for phytoplankton community composition at Station B. The thick black line is the monthly mean of chl-*a* at Station B. The other lines represent the monthly mean chl-*a* associated with the major phytoplankton groups, diatoms (open triangle-dotted line), cryptophytes (black triangle and solid line), type-4 haptophytes (open diamond-dotted line), and mixed flagellates (grey diamond and grey solid line). The vertical lines represent the monthly standard deviations over the twenty-year time series. (For interpretation of the references to color in this figure legend, the reader is referred to the web version of this article).

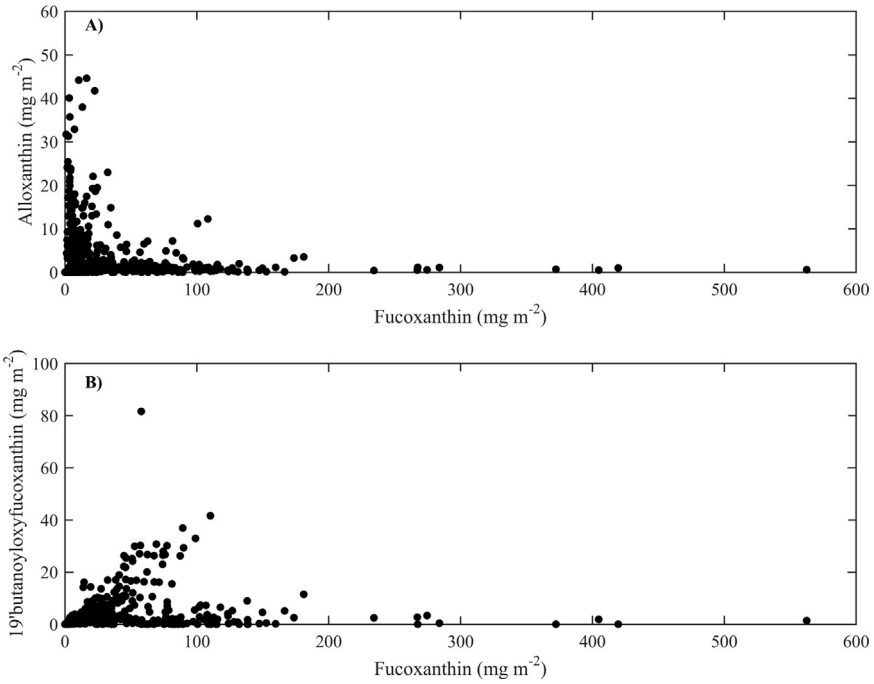

Fig. 9. The relationship between the major phytoplankton contributors (diatoms, cryptophytes, and mixed flagellates) to the chl-*a* at Station E. A) The relationship between water column integrated concentrations of alloxanthin (mg m^{-2}, cryptophytes) and fucoxanthin (mg m^{-2}, diatoms) at Stations B and E. B) The relationship between concentrations of 19′-butanoyloxyfucoxanthin (mg m^{-2}, major marker pigment for mixed flagellates) and fucoxanthin (mg m^{-2}, diatoms) at Stations B and E.

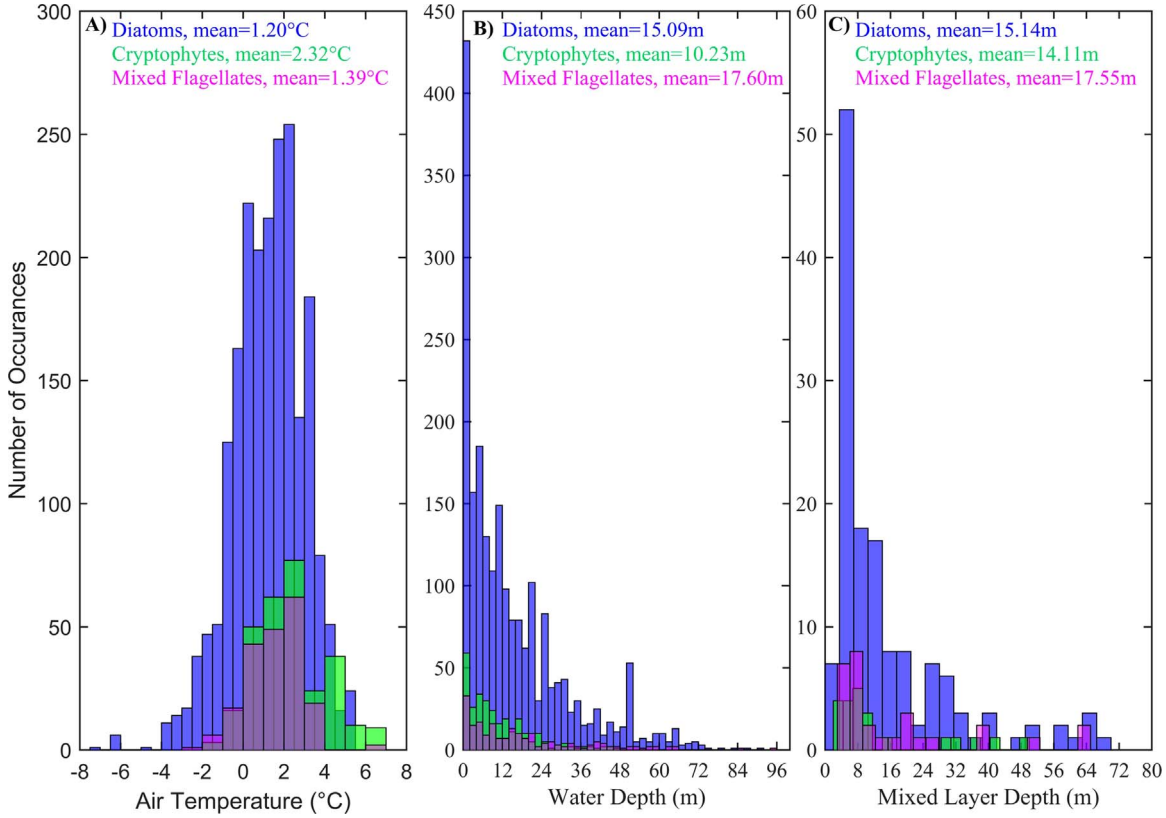

Fig. 10. Frequency of observations of specific taxa when greater than 50% of the chl-*a* against atmospheric air temperature, water depth and mixed layer depth. A) The frequency of observations where water column chl-*a* concentrations were dominated by either diatoms, cryptophytes, and mixed flagellates. B) The frequency of observations where chl-*a* concentrations were dominated by either diatoms, cryptophytes, and mixed flagellates as a function of water column depth. C) The frequency of observations where chl-*a* concentrations were dominated by either diatoms, cryptophytes, and mixed flagellates as a function of mixed layer depth. Data does not include depth when no stratification was observed (see methods and Carvalho et al. (2017)).

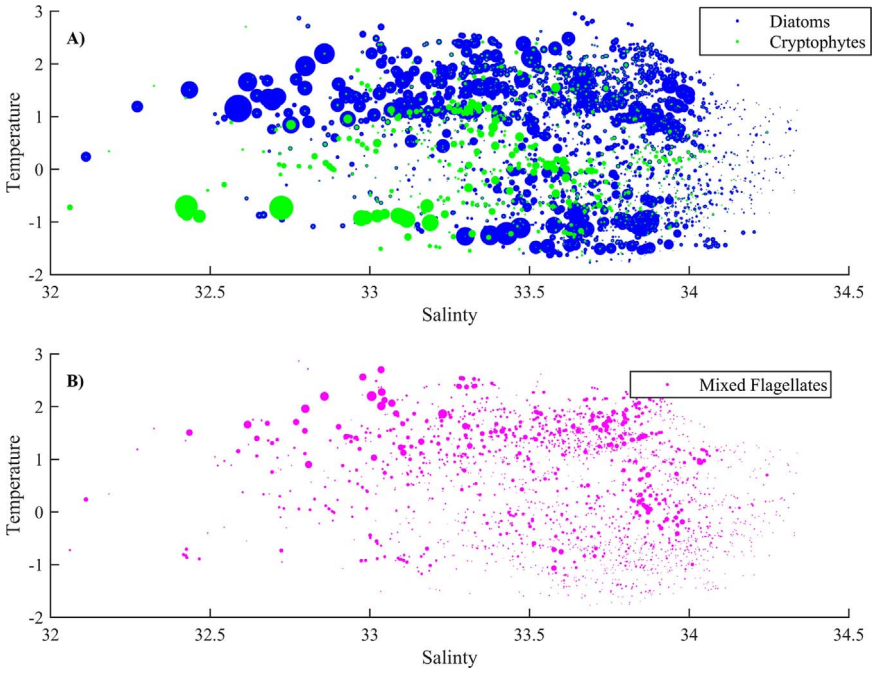

Fig. 11. The presence of the major phytoplankton taxa plotted in temperature and salinity phase space. The size of the circles indicates the relative concentration of chl-*a* for the discrete samples collected at Stations B and E. A) The relative presence offucoxanthin (blue = diatoms) and alloxanthin (green = cryptophytes) plotted in temperature and salinity space. B) The relative presence of mixed flagellates (pink) in temperature salinity space. (For interpretation of the references to color in this figure legend, the reader is referred to the web version of this article).

in the following spring and summer (Vernet et al., 2008). The key observation is that the depth of the summer mixed layer depth and the length of the summer growing season (defined by the number of ice free days) are the critical factors driving the size of the summer phytoplankton blooms at Palmer Station.

Highest concentrations and the inter-annual variability in chl-*a* were associated with the dynamics in diatoms and cryptophytes (Fig. 11). Mixed flagellates showed limited interannual variability but were a consistent component to the overall phytoplankton population. Diatom blooms accounted for the largest phytoplankton blooms in the region and the highest chl-*a* concentrations were associated with shoaling seasonal mixed layer depths in the summer (Carvalho et al., 2016), while cryptophytes blooms occurred during the summer and were associated with glacial melt-water after sea ice retreat. This is in agreement with other studies (Moline et al., 2004; Kozlowski et al., 2011; Mendes et al., 2013). Time series measurements collected by the Rothera Oceanographic and Biological Time Series (Clarke et al., 2008a, 2008b) to the south of Palmer Station in Marguerite Bay has also documented the importance of diatoms and cryptophytes; however unlike this study there was also a significant presence of haptophytes (Rozema et al., 2016). In those waters to the south, cryptophytes and haptophytes were correlated with the deep winter and early spring mixed layer, suggesting they were the dominant resident phytoplankton until the mixed layer shallowed when large diatoms then grew to dominate the summer phytoplankton populations (Rozema et al., 2016). This is in contrast to our site where cryptophytes increased only during peak summer months; however it should be noted the sampling for our program starts during the summer and we have limited winter/early spring data. Rozema et al. (2016) observed that cryptophytes were also found in shallower mixed layers in the summer especially during summers of lower chl-*a* biomass, which was associated lower diatom abundances. This is consistent with our findings.

These time series sites highlights the need for a physiological characterization of Antarctic cryptophytes to allow for a robust under-

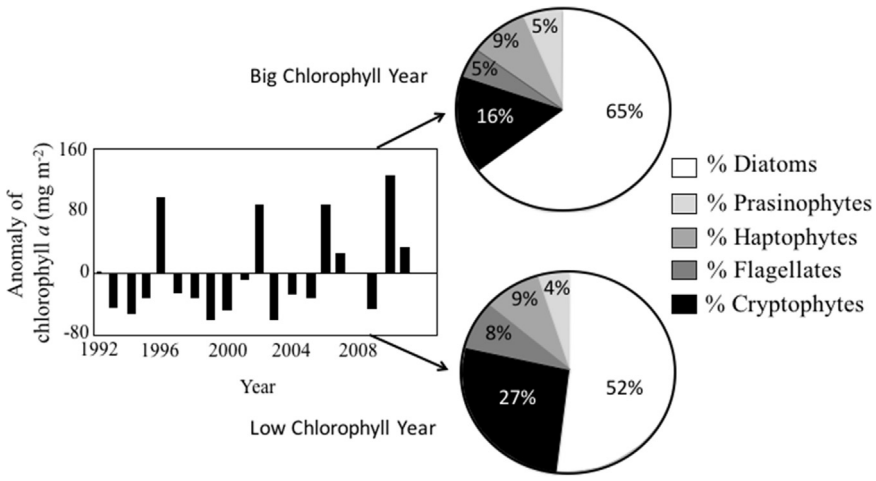

Fig. 12. The dynamics associated with years of high and low phytoplankton biomass as indicated by chl-a anomalies (calculated as described in Saba et al. (2014)) and the relative abundance, calculated from CHEMTAX, for the major phytoplankton taxa over the full summer season.

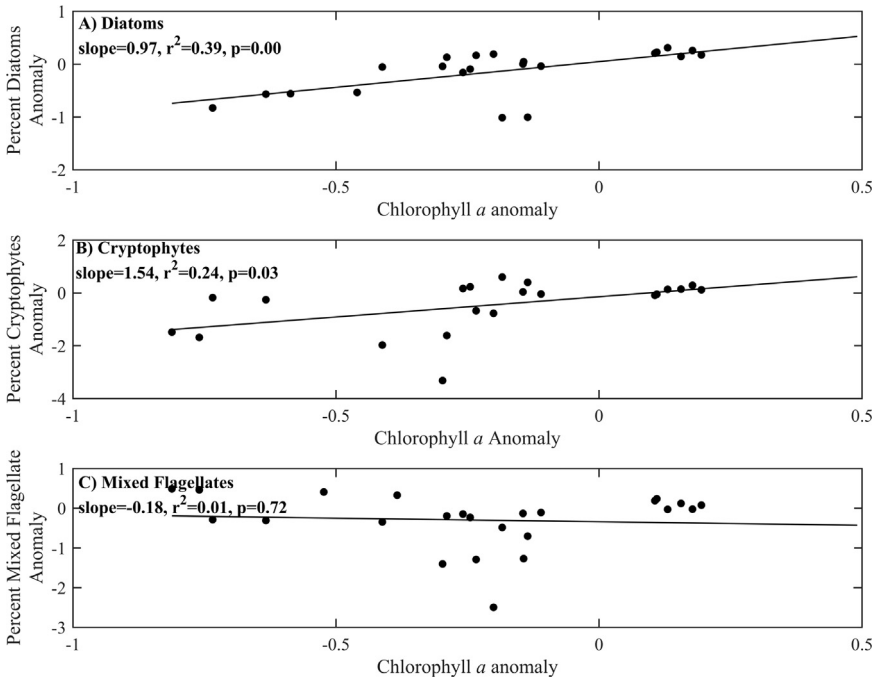

Fig. 13. Correlations between the major phytoplankton taxa contributing to overall chl-*a* concentrations. A) The correlation between anomaly of the relative chl-*a* by the diatoms calculated by CHEMTAX, and the chl-*a* anomaly for summer season (mean calculated over the December-January-February). B) The correlation between the anomaly of the relative chl-*a* by the cryptophytes calculated by CHEMTAX, and the chl-*a* anomaly for summer season (mean calculated over the December-January-February). C) The correlation between anomaly of the relative chl-*a* by the mixed flagellates calculated by CHEMTAX, and the chl-*a* anomaly for summer season (mean calculated over the December-January-February).

standing of their ecology likely at a species level as opposed to a HPLC-taxon specific view. In the Southern Ocean, significant focus has been directed to understanding the physiological ecology of diatoms and *Phaeocystis antarctica* given of their biogeochemical significance; however the amount of research focused on Antarctic cryptophytes is scant. This is problematic as this study complements other work that demonstrates that cryptophytes are a critical component to the algal communities along the West Antarctic Peninsula (Mura and Agusti,1998; Garibotti et al., 2003; F. Rodriguez et al., 2002a; J. Rodriguez et al., 2002b; Moline et al., 2004; Garibotti et al.,2005; Kozlowski et al., 2011; Rozema et al., 2016). Additionally, there is a significant lack of understanding of their ecology due to limited seasonal sampling and gaps in basic biological understanding as only few Southern Ocean cryptophytes are available in culture (*Geminigera cryophyla*). Cryptophytes are cosmopolitan thriving in oligotrophic waters (Ilmavirta, 1988), the Southern Ocean (Fiala et al., 1998), coastal waters (Tamigneaux et al., 1995), estuaries (Pinckney et al., 1998), and inland lakes (Klaveness, 1988; Higashi and Seki, 2000). The crypotphytes are bi-flagellated autotrophic algae however a significant number are mixotrophic (Davis and Sieburth, 1984; Hill and Rowan, 1989). The mixotrophic nature has been hypothesized to allow cells to supplement photosynthesis to allow them to thrive in the dim light conditions found at depth where they often reside (Ilmavirta, 1988; Bergmann et al., 2004). This is consistent with the observation that cryptophytes appear to be highly sensitive to high intensity visible and ultraviolet radiation as they are not able to produce photoprotective compounds to protect cellular machinery damaging irradiances (Vernet et al., 1994). In response to increased levels of ultraviolet radiation cryptophytes exhibit a decrease in motility and carbohydrate reserves and bleaching of pigments (Plante and Arts, 2000). The cryptophytes in these waters in West Antarctic peninsula appear to be distinct from many other ocean regions as cryptophyte populations are often confined in the upper water column in the lower salinity surface water (J. Rodriguez et al., 2002b; Moline et al., 2004). The surface populations would be exposed to higher visible and ultraviolet radiation, which should be inhibiting however they appear to thrive. As the cryptophyte blooms do not occur in high salinity waters with a deep upper mixed layer depth, it is unlikely that light limitation serves as the critical factor influencing cryptophyte bloom initiation. This suggests the low salinity water provides either a specific micronutrient and/or alleviation from microzooplankton grazing.

Antarctic coastal waters are highly productive with a short summer growing season initiated when light levels are sufficiently high to support photosynthesis (Smith et al., 1996, 1999; Smith and Gordon, 1997; Arrigo et al., 1998; Vernet et al., 2008). The phytoplankton productivity supports an extensive food web with krill as a keystone trophic link between primary producers and top predators (McWhinnie and Denys, 1980; Valiela, 1995). The interannual variability in the summer diatom productivity in the WAP (Ducklow et al., 2012) is associated with krill recruitment (Saba et al., 2014), which is consistent with the Antarctic paradigm of a short diatom − krill − top predator food chain. In summer seasons with lower phytoplankton biomass there is an enhanced proportion of the chl-*a* being associated with cryptophytes, which represents a shift in the overall size spectrum of the primary producers. Bloom-forming diatoms range in size from 15 to 270 μm (Kopczynska, 1992; Moline and Prézelin, 1996), while the Antarctic cryptophytes have been measured microscopically to be 8 ± 2 μm (McMinn and Hodgson, 1993). The shift in the nature of the phytoplankton community suggests the importance of regenerated communities in the WAP, which is consistent with other studies that have stressed the importance of microzooplankton grazing on smaller size phytoplankton (Hewes et al., 1985; El Sayed, 1988; Daniels et al., 2006; Garzio et al., 2013). These results agree with data collected ~500 km to the south as part of the Rothera Antarctic Time Series (Clarke et al., 2008a, 2008b) south that has also recently documented that reduced winter sea ice cover leads to low phytoplankton biomass and enhanced proportions of nanophytoplankton (Rozema et al., 2016).

The increase in the importance of the productivity associated with smaller cells during low chl-*a* years is consistent with inverse food web modeling results that suggest that the northern WAP is not always dominated by the diatom − krill − apex predator food chain (Sailley et al., 2013). Micrograzers can play a significant role with ingestion

rates up to double the amount of carbon ingested by krill and carbon flow through bacteria being equivalent to ~75% of the carbon ingested by krill. This to a certain extent reflects the poor clearance rate efficiencies of krill for smaller phytoplankton cells such as the cryptophytes (< 10 μm, Meyer and El-Sayed, 1982; Boyd et al., 1984; Quetin and Ross, 1985; Weber and El-Sayed, 1987). Measured grazing rates of krill on cryptophytes are negligible (Haberman et al., 2003). Inverse model results suggest microzooplankton can make up 10–70% of the total carbon ingested by krill (Sailley et al., 2013), which is consistent with observations that krill gut contents can contain 20–80% microzooplankton (gut volume; Perissinotto et al., 2000). The importance of the microzooplankton in krill diets is variable as the overall amount of microzooplankton ingested varies with the fraction of large phytoplankton that are available to krill, with micro-zooplankton supplementing krill metabolic needs when fewer large phytoplankton are present (Bernard et al., 2012). This lead Sailley et al. (2013) to propose the WAP food web was oscillating from a fully herbivorous food web with krill as the dominant grazer, and a microbial food web where microzooplankton grazing and bacterial production are more important. The results of Saba et al. (2014) and this study support this view, with periodic high productivity diatom-dominated years associated with specific environmental conditions eliciting an immediate response in krill recruitment followed by a series of lower productivity years associated with lower krill recruitment. The switch to a multivorous community provides sufficient food for the krill population to mature (Saba et al., 2014) despite lower biomass and an overall smaller sized phytoplankton communities. Ensuring a stable community over time would require periodic high productivity diatom summers to ensure high krill fecundity to replenish the aging populations.

The Palmer 20-year *in situ* time series detects an overall increase in the concentration of chl-*a* but not a trended shift composition of the phytoplankton in the waters near Palmer Station due to the high internanual variability of the system. The declines in chl-*a*, in the northern region of the WAP, have been associated with increased wind forcing and cloud cover that together presumably resulted in increased light limitation of phytoplankton (Mitchell and Holm-Hansen, 1991; Moline et al., 1998; Montes-Hugo et al., 2009). Similar north and south differences were identified by Sailley et al. (2013) whose inverse models suggest that the Southern region of the WAP remained a short diatom − krill − top predator food chain while the Northern WAP was largely multivorous. Consistent with this study, the 3-decade satellite ocean color study also detected a decrease in the overall particle size spectrum in regions where phytoplankton biomass had declined (Montes-Hugo et al., 2009). This is consistent with historical data that shows nanoplankton are inversely related to overall watercolumn density (Whitaker, 1982; Krebs, 1983; Rozema et al., 2016) and would be associated with the increased presence of sea ice and glacial melt over time. Recent changes since 2009 showed increasing sea ice and with it increased chl-*a* concentrations suggesting that ecosystem can rebound quickly; however if long term decadal predictions hold that current warming and wind intensification will resume, the corresponding deeper mixing, lower biomass and smaller-sized phytoplankton communities in the Palmer Station region would have detrimental impacts on higher trophic levels dependent on a krill-dominated food web.

Acknowledgements

We thank Raytheon Polar Services and Lockheed Martin, the captains and crews of the R.V. Laurence M. Gould, and the Palmer Station crew for field assistance. We thank the many current and former PAL-LTER team members for their excellence in the field and laboratory. The research was supported by the LTER Program of the US National Science Foundation (ANT-0823101). Data from the PAL-LTER data repository were supported by Office of Polar Programs, NSF Grants OPP-9011927, OPP-9632763 and OPP-0217282. We also are grateful from funding provided by NASA Award NNX14AL86G. We also thank two anonymous reviewers whose constructive suggestions improved this manuscript.

References

Arrigo, K., Worthen, D., Schnell, A., Lizotte, M., 1998. Primary production in southern ocean waters. J. Geophys. Res. Oceans 103, 15587–15600.

Bergmann, T., Fahnensteil, G., Lohrenz, S., Millie, D.F., Schofield, O., 2004. The effect of a spring turbidity event on spectral light fields and phytoplankton community dynamics. J. Geophys. Res. 109 (No. C10), C10S15. http://dx.doi.org/10.1029/2002JC001575.

Bernard, K.S., Steinberg, D.K., Schofield, O., 2012. Summertime grazing impact of the dominant macrozooplankton off the Western Antarctic Peninsula. Deep-Sea Res. I 62, 111–122.

Boyd, C.M., Heyraud, M., Boyd, C.N., 1984. Feeding of the Antarctic krill, *Euphausia superba*. Crustace. Biol. 4, 123–141.

Buma, A.G.J., de Baar Nolting, H.J.W., van Bennekom, R.F., 1991. Metal enrichment experiments in the Weddell–Scotia seas: effects of Fe and Mn on various plankton communities. Limnol. Oceanogr. 36, 1865–1878.

Carvalho, F., Kohut, J., Oliver, M.J., Sherrell, R.M., Schofield, O., 2016. Mixing and phytoplankton dynamics in a submarine canyon in the West Antarctic Peninsula. J. Geophys. Res. http://dx.doi.org/10.1002/2016JC011650.

Carvalho, F., Kohut, J., Oliver, M.J., Schofield, O., 2017. Defining the ecologically relevant mixed-layer depth for Antarctica's coastal seas. Geophys. Res. Lett. 44. http://dx.doi.org/10.1002/2016GL071205.

Clarke, A., Meredith, M.P.M., Wallace, M.I., Brandon, A., Thomas, D.N., 2008a. Seasonal and interannual variability in temperature, chlorophyll, and macronutrients in the northern Marguerite Bay, Antarctica. Deep-Sea Res. Part II 55, 1988–2006. http://dx.doi.org/10.1016/j.dsr2.2008.04.035.

Clarke, A., Murphy, E.J., Meredith, M.P., King, J.C., Peck, L.S., Barnes, D.K.A., Smith, R.C., 2007. Climate change and the marine ecosystem of the western Antarctic Peninsula. Philos. Trans. R. Soc. Lond. B 362, 149–166. http://dx.doi.org/10.1098/rstb.2006.1958.

Clarke, A., Meredith, M.P., Wallace, M.I., Brandon, M.A., Thomas, D.N., 2008b. Seasonal and interannual variability in temperature, chlorophyll and macronutrients in northern Marguerite Bay, Antarctica. Deep-Sea Res. Part II 55, 1988–2006. http://dx.doi.org/10.1016/j.dsr2.2008.04.035.

Fox, Cook A.J., Vaughan, A.J., Ferrigno, J.G, D.G., 2005. Retreating glacier fronts on the antarctic Peninsula over the past half-century. Science 308, 541–544.

Daniels, R.M., Richardson, T.L., Ducklow, H.W., 2006. Food web structure and biogeochemical processes during oceanic phytoplankton blooms: an inverse model analysis. Deep-Sea Res. II 53, 532–554.

Davis, P., Sieburth, J., 1984. Estuarine and oceanic microflagellate predation of actively growing bacteria: estimation by frequency of dividing-divided bacteria. Mar. Ecol. Progress Ser. 19, 237–246.

Ducklow, H.W., Baker, K., Martinson, D.G., Quetin, L.B., Ross, R.M., Smith, R.C., Stammerjohn, S.E., Vernet, M., Fraser, W., 2007. Marine ecosystems: the West Antarctic Peninsula. Philos. Trans. R. Soc. Lond. B 362, 67–94.

Ducklow, H., Clarke, A., Dickhut, R., Doney, S.C., Geisz, H., Huang, K., Martinson, D.G., Meredith, M.P., Moeller, H.V., Montes-Hugo, M., Schofield, O., Stammerjohn, S.E., Steinberg, D., Fraser, W., 2012. Marine pelagic ecosystems: the West Antarctic Peninsula. In: Rogers, A.D. (Ed.), Antarctica: An Extreme Environment in a Changing World. Wiley.

El-Sayed, S., 1988. Productivity of the southern ocean: a closer look. Comp. Biochem. Physiol. B 90, 489–498.

Fiala, M., Semeneh, M., Oriol, L., 1998. Size-fractionated phytoplankton biomass and species composition in the Indian sector of the Southern Ocean during austral summer. J. Mar. Syst. 17, 179–194.

Garibotti, I.A., Vernet, M., Ferrario, M.E., Smith, R.C., Ross, R.M., Quetin, L.B., 2003. Phytoplankton spatial distribution patterns along the Western Antarctic Peninsula (Southern Ocean). Mar. Ecol. Progress. Ser. 261, 21–39.

Garibotti, I.A., Vernet, M., Ferrario, M.E., 2005. Annually recurrent phytoplanktonic assemblages during summer in the seasonal ice zone west of the Antarctic Peninsula (Southern Ocean). Deep-Sea Res. II 52, 1823–1841. http://dx.doi.org/10.1016/j.dsr.2005.05.003.

Garzio, L.M., Steinberg, D.K., 2013. Microzooplankton community composition along the Western Antarctic Peninsula. Deep Sea Res. I 77, 36–49. http://dx.doi.org/10.1016/j.dsr.2013.03.001.

Haberman, K.L., Ross, R.M., Quetin, L.B., 2003. Diet of Antarctic krill (*Euphausia superba Dana*): II. Selective grazing in mixed phytoplankton assemblages. J. Exp. Mar. Biol. Ecol. 283, 97–113.

Hart, T.J., 1942. Phytoplankton periodicity in Antarctic surface waters. Discov. Rep. 21, 261–356.

Hewes, C., Sakshaug, E., Holm-Hansen, O., 1985. Alternative pathways at lower trophic levels in the Antarctic food web. In: Siegfried, W., Condy, P., Laws, R. (Eds.), Antarctic Nutrient Cycles and Food Webs. Springer, Berlin, pp. 277–283.

Hewes, C.D., Sakshaug, E., Reid, F.M.H., Holm-Hansen, O., 1990. Microbial autotrophic and heterotrophic eucaryotes in Antarctic waters: relationships between biomass and chlorophyll, adenosine triphosphate and particulate organic carbon. Mar. Ecol. Progress Ser. 63, 27–35.

Higashi, Y., Seki, H., 2000. Ecological adaptation and acclimatization of natural freshwater phytoplankters with a nutrient gradient. Environ. Pollut. 109, 311–320.

Hill, D., Rowan, K., 1989. The biliproteins of the *Cryptophyceae*. Phycologia 28 (4), 455–463.

Holm-Hansen, O., Mitchell, B.G., 1991. Spatial and temporal distribution of phytoplankton and primary production in the western Bransfield Strait region. Deep-Sea Res. 38, 961–980. http://dx.doi.org/10.1016/0198-0149(91)90092-T.

Ilmavirta, V., 1988. Phytoflagellates and their ecology in Finnish brown water lakes. Hydrobiologia 161, 255–270.
Jacques, G., Panouse, M., 1991. Biomass and composition of size fractionated phytoplankton in the Weddell Sea confluence area. Polar Biol. 11, 315–328. http://dx.doi.org/10.1007/BF00239024.
Kim, H., Doney, S.C., Iannuzzi, R.A., Meredith, M.P., Martininson, D.G., Ducklow, H.W., 2016. Climate forcing for dynamics of dissolved inorganic nutrients at Palmer station, Antarctica: an interdecadal (1993–2013) analysis. J. Geophys. Res.: Biogeosciences 12. http://dx.doi.org/10.1002/2015JG003311.
Klaveness, D., 1988. Ecology of the *Cryptomonadida*: A First Review. Growth and Reproductive Strategies of Freshwater Phytoplankton. (C. Sandgren) Cambridge University Press, New York, pp. 105–133.
Klinck, J.M., 1998. Heat and salt changes on the continental shelf west of the Antarctic Peninsula between January '93 and January '94. J. Geophys. Res. 103b, 7617–7636. http://dx.doi.org/10.1029/98JC00369.
Kopczynska, E.E., 1992. Dominance of microflagellates over diatoms in the Antarctic areas of deep vertical mixing and krill concentrations. J. Plankton Res. 14, 1031–1054.
Kozlowski, W.A., Deutschman, D., Garibotti, I., Trees, C., Vernet, M., 2011. An evaluation of the application of CHEMTAX to Antarctic coastal pigment data. Deep-Sea Res. I 58, 350–364.
Krebs, W.N., 1983. Ecology of neritic marine diatoms, Arthur Harbor, Antarctica. Micropaleontology 29, 267–297.
Lorbacher, K., Dommenget, D., Niiler, P.P., Köhl, A., 2006. Ocean mixed layer depth: a subsurface proxy of ocean-atmosphere variability. J. Geophys. Res. 111, C07010. http://dx.doi.org/10.1029/2003JC002157.
Martinson, D.G., Stammerjohn, S.E., Iannuzzi, R.A., Smith, R.C., Vernet, M., 2008. Western Antarctic Peninsula physical oceanography and spatio-temporal variability. Deep Sea Res. II 55, 1964–1987.
McMinn, A., Hodgson, D., 1993. Summer phytoplankton succession in Ellis Fjord, eastern Antarctica. J. Plankton Res. 15, 925–938.
McWhinnie, M.A., Denys, C.J., 1980. The high importance of the lowly krill. Nat. Hist. 89, 66–73.
Mendes, C.R.B., Tavano, V.M., Leal, M.C., de Souza, V., Brotas, M.S., Garcia, C.A.E., 2013. Shifts in the dominance between diatoms and cryptophytes during three late summers in the Bransfield Strait (Antarctic Peninsula). Polar Biol. 36, 537–547. http://dx.doi.org/10.1007/s00300-012-1282-4.
Meyer, M.A., El-Sayed, S.Z., 1982. Grazing of Euphausia superba Dana on natural phytoplankton populations. Polar Biol. 4, 193–197. http://dx.doi.org/10.1007/BF00443187.
Mitchell, B.G., Holm-Hansen, O., 1991. Observations and modeling of the Antarctic phytoplankton crop in relation to mixing depth. Deep-Sea Res. 38, 981–1007.
Moline, M.A., Prézelin, B.B., 1996. Palmer LTER 1991–1994: long-term monitoring and analyses of physical factors regulating variability in coastal Antarctic phytoplankton biomass, *in situ* productivity and taxonomic composition over subseasonal, seasonal and interannual time scales. Mar. Ecol. Progress Ser. 145, 143–160.
Moline, M.A., Schofield, O., Boucher, N.B., 1998. Photosynthetic parameters and empirical modeling of primary production in the Southern ocean. Antarct. Sci. 10, 45–54.
Moline, M.A., Claustre, H., Frazer, T.K., Schofield, O., Vernet, M., 2004. Alteration of the food web along the Antarctic Peninsula in response to a regional warming trend. Glob. Change Biol. 10, 1973–1980.
Montes-Hugo, M., Doney, S.C., Ducklow, H.W., Fraser, W., Martinson, D., Stammerjohn, S.E., Schofield, O., 2009. Recent changes in phytoplankton communities associated with rapid regional climate change along the Western Antarctic Peninsula. Science 323, 1470–1473.
Mura, M.P., Satta, M.P., Agusti, S., 1995. Water-mass influences on summer Antarctic phytoplankton biomass and community structure. Polar Biol. 15, 15–20.
Mura, M.P., Agusti, S., 1998. Increased frequency of dividing cells of a phototrophic species of Cryptophyceae at a frontal structure off the Antarctic Peninsula. J. Plankton Res. 20 (12), 2357–2367.
Nelson, D.M., Smith, W.O., 1991. Sverdrup revisited: critical depths, maximum chlorophyll levels, and the control of Southern Ocean productivity by the irradiance-mixing regime. Limnol. Oceanogr. 36, 1650–1661.
Oliver, M.A., Irwin, A., Moline, M.A., Fraser, W., Patterson, D., Schofield, O., Kohut, J., 2013. Adelie penguin foraging location correlated with local tides. PLoS One E55163. http://dx.doi.org/10.1371/journal.pone.0055163.
Perissinotto, R., Gurney, L., Pakhomov, E.A., 2000. Contribution of heterotrophic material to diet and energy budget of Antarctic krill *Euphausia superba*. Mar. Biol. 136, 129–135.
Pinckney, J., Paerl, H., Harrington, M., Howe, K., 1998. Annual cycles of phytoplankton community-structure and bloom dynamics in the Neuse River Estuary, NC. Mar. Biol. 131, 371–381.
Plante, A., Arts, M., 2000. Effects of chronic, low levels of UV radiation on carbon allocation in *Cryptomonas erosa* and competition between *C. erosa* and bacteria in continuous cultures. J. Plankton Res. 22 (7), 1277–1298.
Prézelin, B.B., Hofmann, E.E., Mengelt, C., Klinck, J.M., 2000. The linkage between upper circumpolar deep water (UCDW) and phytoplankton assemblages on the west Antarctic Peninsula Continental Shelf. J. Mar. Res. 58, 165–202.
Prézelin, B.B., Hofmann, E.E., Moline, M., Klinck, J.M., 2004. Physical forcing of phytoplankton community structure and primary production in continental shelf waters of the Western Antarctic Peninsula. J. Mar. Res. 62, 419–460.
Quetin, L.B., Ross, R.M., 1985. Feeding by Antarctic krill, Euphausia superba: does size matter? In: Webs, Siegfried, W.R., Condy, P.R., Laws, R.M. (Eds.), Antarctic Nutrient Cycles and Food. Springer-Verlag, Berlin, pp. 372–377.
Rignot, E., Bamber, J.L., Van den Broeke, 2008. Recent Antarctic ice mass loss from radar interferometry and regional climate modeling. Nat. Geosci. 1, 106–110.
Rodriguez, F., Varela, M., Zapata, M., 2002a. Phytoplankton assemblages in the Gerlache and Bransfield Straits (Antarctic Peninsula) determined by light microscopy and CHEMTAX analysis of HPLC pigment data. Deep Sea Res. Part II. 49, 723–747.
Rodriguez, J., Rodriguez, J.-G., Blanco, J.M., Figueroa, F.L., 2002b. Physical gradients and spatial variability of the size structure and composition of phytoplankton in Gerlache Strait (Antarctica). Deep-Sea Res. II 49, 693–706.
Rozema, P.D., Venables, H.J., van de Poll, W.H., Clarke, A., Meredith, M.P., Buma, A.J.A., 2016. Interannual variability in phytoplankton biomass and species composition in northern Marguerite Bay (West Antarctic Peninsula) is governed by both winter sea ice cover and summer stratification. Limnol. Oceanogr. http://dx.doi.org/10.1002/lno.10391.
Saba, G.K., Fraser, W.R., Saba, V.S., Iannuzzi, R.A., Coleman, K.E., Doney, S.C., Ducklow, H.W., Martinson, D.G., Miles, T.N., Patterson-Fraser, D.L., Stammerjohn, S.E., Steinberg, D.K., Schofield, O., 2014. Winter and spring controls on the summer food web of the coastal West Antarctic Peninsula. Nat. Commun. 5, 4318. http://dx.doi.org/10.1038/ncomms5318.
Sailley, S., Ducklow, H.W., Moeller, H.V., Fraser, W.R., Schofield, O., Steinberg, D.K., Garzio, L.N., Doney, S.C., 2013. Carbon fluxes and pelagic ecosystem dynamics near two western Antarctic Peninsula Adelie penguin colonies: an inverse model approach. Mar. Ecol. 492, 253–272. http://dx.doi.org/10.3354/meps10534.
Schofield, O., Ducklow, H.W., Martinson, D.G., Meredith, M.P., Moline, M.A., Fraser, W.R., 2010. How do polar marine ecosystems respond to rapid climate change? Science 328, 1520. http://dx.doi.org/10.1126/science.1185779.
Schofield, O., Duclow, H., Bernard, K., Doney, S., Fraser-Patterson, D., Gorman, K., Martinson, D., Meredith, M., Saba, G., Stammerjohn, S., Steinberg, D., Fraser, W., 2013. Penguin biogeography along the West Antarctic Peninsula: testing the canyon hypothesis with Palmer LTER observations. Oceanography 26, 78–80.
Serebrennikova, Y.M., Fanning, K.A., 2004. Nutrients in the Southern Ocean GLOBEC region: variations, water circulation, and cycling. Deep-Sea Res. II 51, 1981–2002. http://dx.doi.org/10.1016/j.dsr2.2004.07.023.
Skvarca, P., Rack, W., Rott, H., 1999. Climatic trend and the retreat and disintegration of ice shelves on the Antarctic Peninsula: an overview. Polar Res. 18, 151–157.
Smith, R.C., Dierssen, H., Vernet, M., 1996. Phytoplankton biomass and productivity in the western Antarctic Peninsula region. In: Ross, R., Hofmann, E., Quetin, L. (Eds.), Foundation for Ecological Research West of the Antarctic Peninsula. American Geophysical Union, Washington, DC, pp. 333–356.
Smith, R.C., Ainley, D., Baker, K., Domack, E., Emslie, S., Fraser, B., Kennet, J., Leventer, A., Mosley-Thompson, E., Stammerjohn, S., Vernet, M., 1999. Marine ecosystem sensitivity to climate change. Bioscience 49 (5), 393–404.
Smith, W.O., Gordon, L.I., 1997. Hyperproductivity of the Ross Sea (Antarctica) polynya during austral spring. Geophys. Res. Lett. 24, 233–236. http://dx.doi.org/10.1029/96GL03926.
Smith, R.C., Martinson, D.G., Stammerjohn, S.E., Iannuzzi, R.A., Ireson, K., 2008. Bellingshausen and Western Antarctic Peninsula region: pigment biomass and sea ice spatial/temporal distributions and interannual variability. Deep-Sea Res. II 55. http://dx.doi.org/10.1016/j.dsr2.2008.04.027].
Stammerjohn, S.E., Martinson, D.G., Smith, R.C., Iannuzzi, R.A., 2008. Sea ice in the western Antarctic Peninsula region: spatio-temporal variability from ecological and climate change perspectives. Deep Sea Res. II 55, 2041–2058.
Tamigneaux, E., Vazquez, E., Mingelbier, M., Kelein, B., Legendre, L., 1995. Environmental control pf phytoplankton assemblages in nearshore marine waters, with special emphasis on phototrophic ultraplankton. J. Plankton Res. 17 (7), 1421–1447.
Thomas, E.R., Marshall, G., McConnell, J.R., 2008. A doubling in snow accumulation in the western Antarctic Peninsula since 1850. Geophys. Res. Lett. 35, L01706 (doi: 0.1029/2007GL032529).
Turner, J., others, 2005. Antarctic climate change during the last 50 years. Int. J. Climatol. 25, 279–294. http://dx.doi.org/10.1002/joc.1130.
Turner, J., Lu, W., White, I., King, J.C., Phillips, T., Hosking, S.J., Bracegirdle, T.J., Marshall, G.J., Mulvaney, R., Deb, P., 2016. Absence of 21st century warming on Antarctic Peninsula consistent with natural variability. Nature 535, 411–415. http://dx.doi.org/10.1038/nature18645.
Valiela, I., 1995. Marine Ecological Processes. Springer, New York, NY.
Varela, M., Fernandez, E., Serrét, 2002. Size-fractionated phytoplankton biomass and primary production in the Gerlache and south Bransfield Straits (Antarctic Peninsula) in austral summer 1995–1996. Deep-Sea Res. Ii. 49, 749–768.
Vaughan, D.G., Marshall, G.J., Connolley, W.M., Parkinson, C., Mulvaney, R., Hodgson, D.A., King, J.C., Pudsey, C.J., Turner, J., 2003. Recent rapid regional climate warming on the Antarctic Peninsula. Clim. Change 60, 243–274.
Venables, H.J., Clarke, A., Meredith, M.P., 2013. Wintertime controls on summer stratification and productivity at the western Antarctic Peninsula. Limnol. Oceanogr. 58 (3), 1035–1047. http://dx.doi.org/10.431/lo2013.58.3.1035.
Vernet, M., Brody, E., Holm-Hansen, O., Mitchell, B.G., 1994. The response of Antarctic phytoplankton to ultraviolet radiation: absorption, photosynthesis, and taxonomic composition. Antarct. Res. Ser. 62, 143–158.
Vernet, M., Martinson, D., Ianuzzi, R., Stammerjohn, S., Kozlowski, S., Sines, K., Smith, R.C., Garibotti, 2008. Primary production within the sea-ice zone west of the Antarctic Peninsula. I. Sea ice, summer mixed layer, and irradiance. Deep-Sea Res. II 55, 2068–2085.
Villafañe, V., Helbling, E.W., Holm-Hansen, O., 1993. Phytoplankton around Elephant Island, Antarctica. Polar Biol. 13, 183–191.
Weber, L.H., El-Sayed, S.Z., 1987. Contributions of the net, nano and picoplankton to the phytoplankton standing crop and primary productivity in the Southern Ocean. J. Plankton Res. 9 (5), 973–994.
Whitaker, T.M., 1982. Primary production of phytoplankton off Signy Island, South Orkneys, the Antarctic. Proc. R. Soc. Lond. 214, 169–189.